Engineering Structures xxx (xxxx) xxx-xxx

Contents lists available at ScienceDirect

Engineering Structures

journal homepage: http://ees.elsevier.com

Collapse behavior of masonry domes under seismic loads: An adaptive NURBS kinematic limit analysis approach

N. Grillanda[a], A. Chiozzi[b], G. Milani[a,*], A. Tralli[b]

[a] Department of Architecture, Built Environment and Construction Engineering ABC, Technical University of Milan, Piazza Leonardo da Vinci 32, 20133 Milan, Italy
[b] Department of Engineering, University of Ferrara, Via Saragat 1, 44100 Ferrara, Italy

ARTICLE INFO

Keywords
Masonry domes
Adaptive kinematic limit analysis
NURBS elements
Vulnerability assessment
Horizontal loads
Historical monuments

ABSTRACT

The ultimate limit state behavior of masonry domes under axisymmetric gravity loads is nowadays well known and it has been proved how a generalization of the thrush line method used successfully for arches is quite effective also in this case. However, the behavior of a dome under horizontal loads, which is important in case of seismic action, becomes incredibly hard to tackle and still remains an open issue.The present paper aims at presenting a fast and reliable automatized kinematic limit analysis approach able to accurately predict the actual behavior of masonry domes subjected to horizontal static loads. The model uses a rough discretization of the dome obtained by means of few rigid-infinitely resistant NURBS generated elements, adapting step by step the initial mesh in order to progressively overlap the element edges (where all dissipation is lumped) with the hinges forming the failure mechanism. The adoption of a rough mesh makes the code extremely fast, much more competitive than a standard FE model, allowing at the same time to approximate the actual geometry and load distributions in an extremely accurate way. The utilization of geometries obtained with laser scanner acquisitions is straightforward and the presence of pre-existing cracks can be accounted for as well. Three complex case studies are analyzed in detail to benchmark the approach proposed, relying into existing domes belonging to the Italian cultural heritage. The first example has the geometrical parameters of a typical late Renaissance dome, the Cathedral of Montepulciano, the second is the dome of Anime Sante church (collapsed during the L'Aquila 2009 earthquake with a paradigmatic failure mechanism) and the last is the dome of Caracalla baths, whose causes of collapse remain still unknown. In all cases inspected, the approach proposed quickly provides collapse accelerations and active failure mechanisms at a fraction of the time needed by non-linear FE analyses, providing interesting hints into the actual behavior of such kind of structures under horizontal loads.

1. Introduction

Masonry domes represent one of the most widespread structural typologies in the historical buildings of both Eastern and Western architecture. Since the majority of them date back to centuries ago, an accurate modeling of their mechanical behavior is of fundamental importance to both correctly evaluate their structural safety under gravity loads and ensure their correct conservation [1,2]. Moreover, a large amount of them is located in seismic areas, and the evaluation of their vulnerability is becoming crucial, at least to establish –after preliminary screening- the priorities to follow in light of a strengthening strategy implementation. Recent strong earthquakes occurred in Italy (Umbria-Marche 1997–98, L'Aquila 2009, Emilia 2012 and Central Italy 2016) have been devastating in this regard, causing collapses and serious damages to several domes. This shows the high vulnerability of such kind of structures, but at the same time stimulates the research to predict the accelerations associated to the activation of a failure mechanism and the mechanism itself, this latter information being paramount for an effective local strengthening.

A dome is a vaulted structure having a circular plan and usually the form of a portion of a sphere. As far as the geometry is concerned, a dome is a surface that can be divided into parallels and meridians. The state of stress under gravity loads is typical of a membrane with curved shape. Under vertical loads, meridian stresses are always compressive, whereas along parallels, stresses are positive in the lower part and negative (with beneficial hooping effect) in the upper portion; in most cases the passage from compressive to tensile stresses occurs between 45 and 60 degrees with reference to the vertical axis [3,4]. Assuming that masonry behaves as either a no-tension (or scarcely resistant under tensile stresses) material, it can be stated that the load-bearing capacity of a masonry dome is typically shape-dependent. When hoop membrane stresses due to self-weight and dead loads exceed the weak ten-

* Corresponding author.
Email address: gabriele.milani@polimi.it (G. Milani)

https://doi.org/10.1016/j.engstruct.2019.109517
Received 4 January 2019; Received in revised form 4 July 2019; Accepted 6 August 2019
Available online xxx

sile strength of masonry, then first damages start to appear, namely cracks along meridians open at the base of the dome, because of the positive stresses present in the lower part along parallels. Such progressive crack propagation is always associated to a dilatation of the drum, which makes the deformed shape of the dome similar to an orange peel. Due to the development of vertical cracks, the dome is thus divided in equally stepped wedges, membrane stresses are only compressive and the dome starts behave like a series of concentric masonry arches along the meridians. This phenomenon is quite common in masonry domes, it does not compromise the structural stability and allows to make predictions on the load carrying capacity by means of a modification of the thrust-line approach used for arches, as suggested for instance by [5], where a dome is divided into arches having a constant thickness.

In such or similar arch schematizations, the presence of horizontal cracks not due to meridian stresses is more dangerous and may denounce the development of a kinematic mechanism that may lead to collapse. In fact, like in a simple masonry arch, the position of the line of thrust changes when the vertical load is increased or the geometry of the dome changes during the formation of meridian cracks, moving from the center of the section to its hedges. When the line of thrust touches the external or internal surface of the dome, an annular flexural hinge develops and in the opposite side a crack opens along the parallels [6–8]. The limit analysis of domes axis-symmetrically loaded is therefore relative simple and the literature available is nowadays abundant [2]; on the other hand, the good behavior of such kind of structures under gravity loads fully justify their wide utilization during the history to bear heavy vertical loads and cover large spans. However, when symmetry is lost, as in the case of seismic actions, the determination of the load bearing capacity becomes extremely difficult. Before to deal with the possible seismic collapse of a dome, we think useful briefly review the way the domes have been analyzed during the centuries, the computational methods with which they are studied nowadays and the scarce literature on their behavior under seismic actions.

The modern history of the calculus of masonry vaults [9] begins with the contributions of the late 1600 s English school (Hooke in 1676 and 1705 and Gregory in 1698) that stated the analogy between the inverted shape of a catenary and a compressed arch. Poleni employed this analogy in 1743 for the consolidation of the dome of St. Peter in Rome. Bouguer (1734), Bossut (1778) and Mascheroni (1785) derived equilibrium equations for masonry domes under vertical axisymmetric loads neglecting circumferential forces, i.e., considering a one-dimensional (1D) behavior, even if they seem to recognize the presence of circumferential stresses. In particular, Bouguer (1734), in his geometrical construction, introduces the circumferential actions among dome slices as a qualitative consideration and seems to be aware of the incapability of masonry of carrying tensile stresses, pointing out that, for spherical domes of uniform thickness subjected to self-weight, circumferential stresses change sign at an angle of 0.904 rad. A considerable improvement in the analysis of spherical masonry domes was achieved when Levy (1888) proposed a graphical analysis aimed at finding the circle on which circumferential forces are zero. Due to the hypothesis of null tensile forces, below this circle the behavior of a masonry dome is, indeed, 1D. Despite later developments in the membrane theory of shells [10] and more generally in elastic shells [11], due the unavoidable need to take into account the scarce tensile strength, recent contributions analyze masonry domes in the context of limit analysis. In the first half of the 20th century, new methods of analysis for the evaluation of the behavior of masonry arches were proposed. Namely, Kooharian [12] and in an exhaustive way Heyman [13], extended to no tension materials and in particular to masonry arches and vaults the limit analysis theorems since developed for plastic material with associated flow rules.

Nowadays it can be stated [14,15] that the modern theory of limit analysis for masonry structures, as formalized by Heyman, is the most suited approach to deeply understand and predict the behavior of masonry structures. Typically, an infinite compressive strength and a no-tension resistance are assumed, two hypotheses that turn out to be quite consistent with the actual masonry behavior. In addition, shear failure is neglected because violates one of the classic limit analysis hypothesis, i.e. the associated flow rule. Considering the aforementioned hypotheses, it appears clear that the no-tension limit analysis problem as stated by Heyman is perfectly suited for arches and vaulted structures in general, where the structure collapses for the formation of a mechanism involving different rigid-blocks mutually connected by flexural hinges where dissipation is negligible. The approach is particularly simple, it can be easily take into account both a limited compressive strength and a non-vanishing tensile resistance without an excessive complication, does not require other specific mechanical parameters and can be handled with computerized methods where geometric issues are the most important.

The diffusion of personal computers occurred in the early 70ths stimulated in the successive decades also the research in the field of computerization of structural analyses for masonry vaulted structures. At present, computational methods can be classified into three broad categories: (1) Thrust network methods, based on the Static Theorem of limit analysis and directly derived from Heyman's approach, (2) Adaptive limit analysis, based on the Kinematic Theorem with a representation of the geometry by means of few NURBS elements, (3) Direct Finite Element methods, in the framework of both nonlinear incremental and limit analysis, (4) Discrete element methods.

As far as the thrust network analysis is concerned, O'Dwyer [16] was probably the first to generalize thrust-line approach outside the analyses of arches, introducing the use of 3D funicular force networks defined in plan. His approach is limited to vertical loads and the layout of the networks is fixed in plan. Even though the fixed network in plan still inherently gives rise to conservative results, these 3D networks give a much better understanding of vaults than the previous simplified analysis that combines one-dimensional thrust line analyses. Starting from O'Dwyer's seminal work, Ochsendorf research group at MIT [17,18] and then Block at ETHZ introduced Maxwell reciprocal force diagrams, which describe the possible equilibria of compressive funicular networks, named thrust networks, under vertical loading. A modified approach possibly suitable in presence of horizontal loads has been recently proposed in Italy by different research groups, probably the first one being provided by [19]. A related approach to TNA for generating funicular networks in the presence of vertical loading has been proposed by [20,21], as a specific 3D extension of the lumped stress method. It can be shown how their equilibrium conditions were entirely equivalent to thrust network analysis; in contrast, this approach, based on the discretization of Airy stress functions, presented some challenges with respect to singularities in the boundary conditions and loading, or discontinuities, such as cracks or openings, in the discretized equilibrium surfaces and the supports [21].

Adaptive limit analysis (second approach) is an interesting alternative, because it does not require any kind of expertise by the user and can run assuming different strength hypotheses for the masonry material, including anisotropy, limited shear strength and non negligible tensile strength (this latter assumption being particularly important for the limit analyses of domes made by Roman concrete). The Authors of this paper formalized in [22] an adaptive limit analysis, which is based on the kinematic theorem and requires only a rough discretization of the structure by means of few NURBS described rigid infinitely resistant elements. A given masonry vault, eventually strengthened with tie-rods or FRP, can be geometrically represented in a very accurate way by few NURBS parametric surfaces. According to the real behavior of a masonry vault/dome near failure, each NURBS is assumed as a rigid body, interconnected with neighboring elements by means of curved flexural hinges, where all possible dissipation is lumped. The approach is capable of well predicting the load bearing capacity of masonry vault of arbitrary shape, if the initial mesh is adjusted adaptively, for instance by means of meta-heuristic algorithms (i.e. Genetic Algorithm GA, Particle Swarm Optimization (PSO), Firefly Algorithm (FA), Prey Predator Algorithm (PPA) etc. see [23]), in order to capture the position of the hinges activating that failure mechanism associated with the minimum of the load carrying capacity. It is worth noting that is possible easily take into account any type of loading condition and boundary constraints, any geometry and the expertise required by the user is minimal, being necessary only the knowledge of a 3D CAD software.

The third approach is represented by direct FE methods. Unsurprisingly, ancient masonry vaults have been studied since long time ago by using the most advanced tools available for structural assessment and nonlinear incremental analyses, i.e. by using FE codes both in the static (pushover analyses) and dynamic fields [2]. Limit analysis combined with FEs can be used as well and both upper and lower bound formulations are available, for instance in [24] and [25], also with attempts to adjust the mesh by means of Sequential Linear Programming [26]. In general, the utilization of a direct FE discretization is not wrong and a deep insight into the actual behavior of masonry curved structure up to collapse can be still obtained. However, the computational burden is usually huge, the user needs a strong theoretical background, and, in case of limit analyses formulations, robust linear programming solvers must be available and for non-linear analyses, the sensitivity of the results to the many input material variables needed is an issue to consider carefully.

The last approach concerns the use of discrete element methods to assess the bearing capacity of masonry vaults, which in the recent years has been successfully applied to many typologies of masonry structures (see e.g. [27,28]).

At present, a number of papers devoted to the limit analysis and non-linear behavior of masonry arches subjected to under horizontal loads are available, both experimental or based on the three aforementioned numerical methodologies, because the computational effort needed is much lower than that required for domes subjected to horizontal loads. In the case of arches, the focus was on both the longitudinal behavior of single arches [29,30], but also on the effects of out of plane rotation of spandrel walls [31,32] and multi-span bridges at collapse [33].

The present paper aims at presenting the application of a fast and reliable automatized kinematic limit analysis approach able to accurately predict the actual behavior at failure of masonry domes subjected to horizontal static loads. According to the second methodology discussed previously for the analysis of curved structures at failure, the model uses a rough discretization of the dome obtained by means of few rigid-infinitely resistant NURBS elements, adapting step by step the initial mesh in order to progressively overlap the element edges (where all dissipation is lumped) with the hinges forming the failure mechanism. The adoption of a rough mesh makes the code extremely fast, much more competitive than a standard FE model, allowing at the same time to approximate the real geometry and load distributions in an extremely accurate way. In addition, the approach can be used by anyone unfamiliar with complex structural analyses computations and FEs theory. The utilization of geometries obtained with laser scanner acquisitions can be easily handled, as well as the presence of pre-existing cracks.

In Section 2, we present concisely the main features of the proposed approach. In Section 3, we firstly validate the proposed formulation studying a prototype dome with the geometrical parameters of a typical late Renaissance dome, the Cathedral of Montepulciano, see [34]. At this aim, we compare our results with those obtained with non-linear incremental analyses performed with a FE commercial code. In more detail, we consider the structure subjected to four distributions of horizontal loads respectively inspired by first mode shape on the horizontal plane and in the vertical direction, constant or mixing them together. The aim is to propose and compare different statically equivalent seismic actions. For validation purposes, again in Section 3, we consider two famous cases of collapsed masonry domes, namely the dome of “Anime Sante” church in L'Aquila collapsed during the 2009 earthquake (in this case a direct validation with the “experimental” behavior is available) and the Calidarium dome belonging to Baths of Caracalla complex in Rome. In this latter case, the dome was made by Roman concrete (i.e. with mechanical properties quite different from those assumed for Medieval masonry) and a realistic hypothesis of the collapse causes is provided, according to the numerical results obtained. In all cases, the collapse failure mechanisms are reproduced satisfactorily in comparison either with the results obtained through demanding FE computations or with the geometric configuration of the still standing parts, which are suggestive of the failure mechanism occurred during the collapse. All simulations performed show the reliability of the simple adaptive approach proposed, confirming that it is convenient to adopt such a kinematic approach to deal with the limit analysis of domes subjected to horizontal loads, instead of pursuing strategies based on the thrust network analysis or direct FE computations, which require experience users and potentially long time to be performed.

2. Limit analysis with adaptive search of the collapse mechanism: Main features and computational advantages

In this Section, the essential features of the adaptive search algorithm of limit analysis adopted to predict the behavior at failure of masonry domes under horizontal loads are recalled. First, we discuss how masonry material is modeled and then the computational features that make the approach fast and efficient are discussed.

As far as the material modelling is concerned, the essentials of the material “masonry” should be taken in account, namely the almost vanishing resistance to tensile stress and the good compressive strength, as suggested by Heyman, as well as the exclusion of sliding between blocks, which would require a more sophisticated mathematical approach to deal with non-associated plasticity.

However, it is worth mentioning the tensile strength is not always exactly null, but quite variable and uncertain. In addition, the resistance to compression is at least an order of magnitude greater but finite, as well as the shear resistance, especially in absence of meaningful normal compression, may result quite low.

Moreover, masonry is typically anisotropic at failure, because it is made by bricks or stone blocks staggered row by row and joined with mortar [15]. Furthermore, in the case of vaulted structures, the texture can vary considerably in the different parts of a single structural element. To reproduce consistently all such aspects, the adoption of an isotropic no-tension material –as done in the thrust network analysis- could result simplistic and suitable homogenization techniques should be preferred, as recommended for instance by Milani and co-workers in [35,36]. The advantages of the utilization of an anisotropic strength domain is also related to the fact that a no tension material can be easily obtained by sending the tensile strength f_t to zero. Typically, when the actual texture of the dome is disregarded, an isotropic behavior with limited tensile strength, cap in compression and frictional behavior, as illustrated in Fig. 1, can be effective without the risk to introduce large inaccuracies. Finally, let us observe that for almost brittle materials, which do not diffuse too much damage in neighboring regions, inelastic deformation concentrates along well-defined yield lines and therefore the assumption of numerical models made by rigid elements and inelastic interfaces may be very effective and more realistic.

Limit analysis theorems hold both under the Heyman’s hypotheses (see [37]) and for a generic rigid plastic material with associated flow

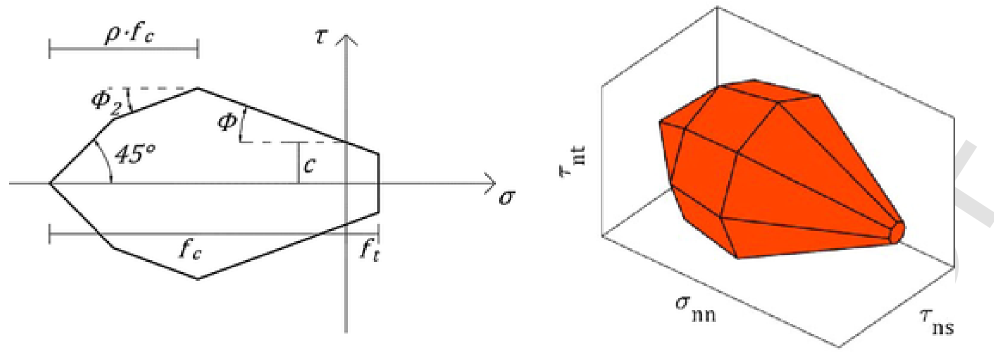

Fig. 1. Typical isotropic strength domain with limited tensile strength, cap in compression and frictional behavior that can be assumed for masonry interfaces in the limit analysis of domes.

rule. However, in presence of friction, the normality rule is lost, because sliding is typically associated to scarce dilation, especially for moderate/strong pre-compression. As well known, in all those cases where the non-associativity can play an important role, see [38] or [39], classic limit analysis does not hold anymore. Robust Linear Programming solvers should be replaced by more demanding Non-Linear Programming approaches, which have been specialized for masonry in different ways by many authors in the recent past, see for instance [40–42]. The effects of friction on the static behavior of masonry vaults has been studied by D'Ayala and coworkers [43,44]. They assert that limit state analysis with finite friction allows investigating two aspects previously neglected for masonry vaults: the possibility of sliding mechanisms between the blocks and the importance of three-dimensional stress fields in the equilibrium of complex vaults. Particularly, the analyses were able to show that for values of the coefficient of friction smaller than 0.5, sliding becomes a critical failure mode and further increases in the thickness are necessary to re-establish equilibrium.

As far as the computational aspects are concerned, three main aspects of the adaptive upper bound limit analysis approach adopted are worth noting, namely:

(1) The "exact" geometrical representation of the dome is obtained with a rough subdivision by means of few rigid NURBS elements. This step is accomplished by subdividing the NURBS two-dimensional parametric space through an *n*-parameters family of straight or curved lines, which are representative of a wide class of physically meaningful mechanisms. The family of subdividing lines is chosen so that, by suitable adjustment of the *n* subdivision parameters (see Step 3), it is capable of capturing mechanisms which closely approximate the actual failure mechanism.
(2) For any mechanism considered, i.e. for each shape of the mesh during the progressive adaptation, the use of efficient internal point algorithms for solving the Linear Programming (LP) problem translating into mathematics the kinematic theorem of limit analysis speeds up considerably the single computations, making the overall algorithm very fast.
(3) The adaptation of the mesh is done step by step using an efficient metaheuristic algorithm, that does not require any information regarding the first derivatives of equality-inequality constraints and objective function.

As for masonry arches, the thrust line shape (in domes the thrust surfaces) and the evaluation of gravity loads depends strictly on the exact determination of the geometry, small differences having significant consequences on the load carrying capacity. Moreover, nowadays laser scanner techniques are commonly used for accurate geometric surveys of complex geometries [45] and to interface with such technology is particularly interesting to have a detailed insight into geometric details that before were usually disregarded.

The NURBS-based approach here adopted interfaces closely with laser scanner surveys, providing very accurate 3D models. In fact, from a laser scanner cloud of points, see e.g. [46], it is possible to generate an accurate NURBS representation of the given vaulted surface, by means of the advanced features found in any commercial free form modeler such as Rhinoceros® [47], see Fig. 2. By exploiting the properties of NURBS functions, a mesh of the given surface, which still provides an exact representation of the vaulted surface, can be obtained. Each element of the mesh is a NURBS surface itself and idealized in the model proposed as a rigid body.

The reader is referred to previous papers by the authors [22,48–51] for an exhausting description of the details of the limit analysis model. Very concisely here the main features of the approach proposed are recalled. NURBS basis functions are built on B-splines basis functions, which are piecewise polynomial functions defined by a sequence of coordinates $\Xi = \{\xi_1, \xi_2, \ldots, \xi_{n+p+1}\}$, also known as the knot

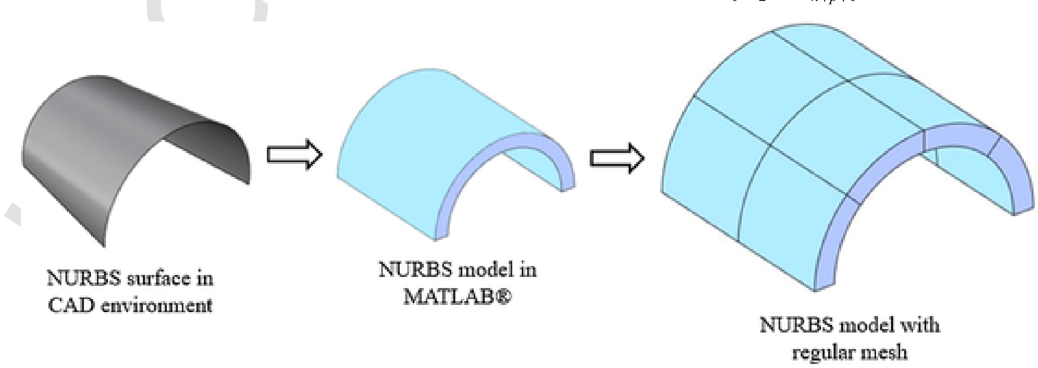

Fig. 2. Passage from NURBS geometric model built in CAD environment (using for instance a laser scanner survey) to the initial NURBS kinematic FE limit analysis discretization.

vector, where the so-called knots, $\xi_i \in [0,1]$, are points in a parametric domain, in which p and n denote the polynomial order and the total number of basis functions, respectively. Once the order of the basis function and the knot vector are known, the i-th B-spline basis function, $N_{i,p}$, can be computed by means of the Cox-de Boor recursion formula [52]. Given a set of weights, $w_i \in R$, the NURBS basis functions, $R_{i,p}$, read as follows:

$$R_{i,p}(\xi) = \frac{N_{i,p}(\xi)w_i}{\sum_{i=1}^{n} N_{i,p}(\xi)w_i}. \quad (1)$$

NURBS share many properties with B-spline basis functions, however they have the great advantage of representing exactly the geometry of a wide set of curves such as circles, ellipses, and parabolas and of all the surfaces that can be generated by such curves.

A NURBS surface of degree p in the u-direction and q in the v-direction is a parametric surface in the three-dimensional Euclidean space defined as follows:

$$\boldsymbol{S}(u,v) = \sum_{i=0}^{n}\sum_{j=0}^{m} R_{i,j}(u,v)\boldsymbol{B}_{i,j} \quad (2)$$

where $\{\boldsymbol{B}_{ij}\}$form a bidirectional net of control points.

Given a NURBS surface$\boldsymbol{S}(u,v)$, isoparametric curves on the surface can be defined by fixing one parameter in the parameter space and letting the other vary. By fixing $u = u_0$ the isoparametric curve $\boldsymbol{S}(u_0, v)$ is defined on the surface $\boldsymbol{S}$, whereas by fixing $v = v_0$ the isoparametric curve $\boldsymbol{S}(u, v_0)$is obtained.

Starting from the geometrical properties of each element, an upper bound formulation can be obtained and implemented through an efficient internal point linear programming algorithm, e.g. using open programming codes as MATLAB, in order to assess the ultimate load bearing capacity of a given masonry dome.

Be N_E the number of elements composing the NURBS mesh, which geometrically represents a generic curved surface. As already pointed out, since each NURBS element is considered rigid and infinitely resistant, the kinematics of each element is determined by the six (three translational and three rotational) generalized velocity components $\{u_x^i, u_y^i, u_z^i, \Phi_x^i, \Phi_y^i, \Phi_z^i\}$ of its center of massG_i, expressed in a global reference system$Oxyz$. On the structure, dead loads $\boldsymbol{F}_0$ and live loads $\boldsymbol{\Gamma}$ are acting. Possible dissipation is assumed to occur only along element interfaces, which are curved splines. Let us observe that is simple to introduce in the structural model a preexisting crack, simply constraining a common edge between two contiguous elements to coincide with the crack.

In order to enforce closely compatibility along interfaces and correctly evaluate the possible dissipated power, integrals are numerically evaluated on interfaces by means of classic collocation method on several points P_i. On each point P_i, a local reference system $(\boldsymbol{n}, \boldsymbol{s}, \boldsymbol{t})$ is defined, where $\boldsymbol{n}$is the unit vector normal to the interface, $\boldsymbol{s}$ is the tangential unit vector in the longitudinal direction and $\boldsymbol{t}$ is the tangential unit vector in the transversal direction, as sketched in Fig. 3.

Taking suitably into account boundary conditions, compatibility constraints and internal and external power dissipation, the upper bound limit analysis problem can be written in compact notation –at freezed discretization or better for each configuration of the mesh used

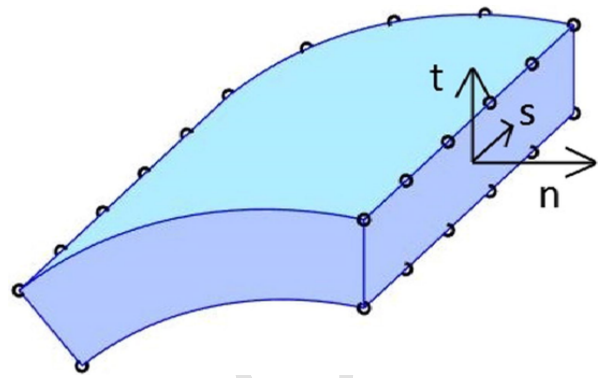

Fig. 3. Collocation method used on curved NURBS edges to correctly approximate expended power and compatibility constraints.

during adaptation- as the following linear programming problem:

$$\begin{cases} \boldsymbol{A}^{eq}\boldsymbol{u} = \boldsymbol{0} & (a) \\ \Delta\tilde{\boldsymbol{u}} = \dot{\lambda}^T \dfrac{\partial f}{\partial \tilde{\boldsymbol{\sigma}}} & (b) \\ \dot{\lambda} \geqslant 0 & (c) \\ P_{\Gamma=1} = 1 & (d) \\ \min\left\{ \Gamma = \dfrac{P_{in} - \boldsymbol{F}_0^T\boldsymbol{u}}{P_{\Gamma=1}} \right\} & \end{cases} \quad (3)$$

In Eq. (3), condition (a) represents the assembled geometrical constraints/boundary conditions, condition (b) compatibility constraints, condition (c) the non-negativity of plastic multipliers and condition (d) normalization of the plastic multiplier.

The progressive adaptation of the mesh is carried out by means of a metaheuristic approach, in order to overlap at the last iteration the position of element edges with fracture lines forming the failure mechanism. Metaheuristic algorithms have a wide range of applicability in the vast structural engineering field, thanks to their efficiency, simplicity of programming, and because they do not require the computation of gradients to linearize constraints and objective function at each iteration. The strength of the proposed method lies in the fact that even by using a mesh made by very few elements, it is possible to obtain an accurate prediction of the load multiplier and active failure mechanism very quickly and without needing a particular expertise by the user.

A recent paper by the Authors [53] is devoted to the evaluation of the most adequate metaheuristic approach to use. The Genetic Algorithm (GA) originally proposed in the first papers [22] has been compared with alternative numerical strategies, as for instance the Particle Swarm Optimization (PSO) Algorithm, the Firefly Algorithm (FA) and a modified version of the Prey-Predator Algorithm (PPA), which turned out to be in general the more efficient and accurate.

Prey-Predator Algorithm (PPA) has been proposed as new algorithm for optimization problems in 2015 by [54]. In this approach, randomly generated solutions are assigned to a predator and preys, depending on their performance in the objective function. This performance is called survival value (SV). The mesh associated with lowest survival value is assigned to the predator and the rest to preys. Then the predator chases the weakest prey, the prey running away from the predator trying to follow the pack of preys with better survival values. The prey with best survival value, which is called the best prey, is considered as a prey which has found a hideout and in this case only a local search is done. The movement of each individual is defined by a direction, i.e. a unit vector, and a step length, which determines how far on that direction the individual tries to move. The reassignment of a predator and preys is repeated at each iteration. In [53] the Authors proposed simplifications related to the specificity of this application and the reader is referred there for further details.

3. Limit analysis of Montepulciano Cathedral dome subjected to vertical and horizontal actions

The first example analyzed is the dome of Montepulciano Cathedral, Fig. 4-a. The example is simplified on purpose, in order to preliminary evaluate the capabilities of the approach proposed in presence of very simple geometries still approximating consistently a real case. The dome is a brick masonry spherical calotte of uniform thickness equal to 15 cm and internal radius equal to 10.60 m. A drum is present under the calotte, whose structural thickness is hard to establish. The drum is then carried by large triumphal arches. Here, the drum thickness is assumed equal to 1 m (corresponding roughly to the continuous core from the top to the bottom), whereas its height is assumed equal to 10.60 m, i.e. equal to the dome radius, see Fig. 4-b. This typical proportion follows classical construction rules adopted during both medieval age and Renaissance. The same example was analyzed by [34] to establish the minimum thickness profile of a dome resting in equilibrium under gravity loads and assuming that masonry behaves as a no-tension material. Openings of the drum and lunettes in the drum crown are not considered for the sake of simplicity. In addition, the actual thickness of the drum crown is not considered and the calotte is prolonged maintaining the constant thickness of the dome. Several FE models are adopted, as shown in Fig. 4-c, namely a NURBS rough discretization to performed the adaptive kinematic limit analysis and two detailed classic FE meshes obtained either with 8-noded brick elements (axis-symmetric) or with 4-noded tetrahedrons (not symmetric because obtained with an auto-meshing routine). The axis-symmetric mesh is used to perform modal analyses and hence apply suitable distributions of horizontal loads when the dome is analyzed under seismic excitation, whereas the discretization with tetrahedron is adopted for the non-linear static analyses.

Mechanical properties adopted in the limit analysis computations are summarized in Table 1 for the NURBS-based limit analysis and Table 2 for the FE non-linear analyses. The main strength parameters have been chosen in agreement with the prescriptions provided by the explicative circular to the Italian Building Code [55,56] for existing buildings. In absence of precise information about the actual texture of the dome, an isotropic failure criterion is adopted. Masonry is assumed behaving as a frictional material with limited tensile strength and linearized cap in compression. Symbols meaning in Table 1 are explained in Fig. 1.

For the FE non-linear static analyses, a total strain cracking model is assumed for masonry, with linear softening in tension and an elastic-perfectly plastic behavior in compression, in agreement with the most diffused approaches used in the literature when a commercial FE code is utilized to perform pushover analyses and more sophisticated approaches accounting for masonry anisotropy cannot be used.

3.1. Calotte under distributed vertical load

When the dome is subjected –apart its own weight- to a distributed vertical load increased up to collapse, the load-displacement curve obtained with the non-linear FE model is that depicted in Fig. 5. Control node is represented by the calotte vertex; as can be noted for an external load equal to zero, a vertical deflection of about 0.8 mm exists, which is due to calotte self-weight. The behavior is elastic up to point A, where the dome detaches from the drum, as demonstrated by the crack pattern reported in Fig. 5. From point A forward, the global behavior is characterized by softening and initial snap-back, both phenomena being explained by the progressive formation of meridian cracks, which are clearly visible at the end of the simulations, i.e. in correspondence of Point B. As a result, the behavior of the dome after the formation of the meridian cracks is highly brittle. The crack pattern obtained at failure is slightly asymmetric because the discretization used is obtained through an auto-meshing pre-processor. In the same figure, collapse loads obtained with limit analysis are also represented assuming for masonry different values of tensile strength and keeping all the other parameters unaltered. As can be observed and as expected, the no-tension material hypothesis is over-conservative, providing an ultimate load bearing capacity roughly reduced by half. In addition, re-

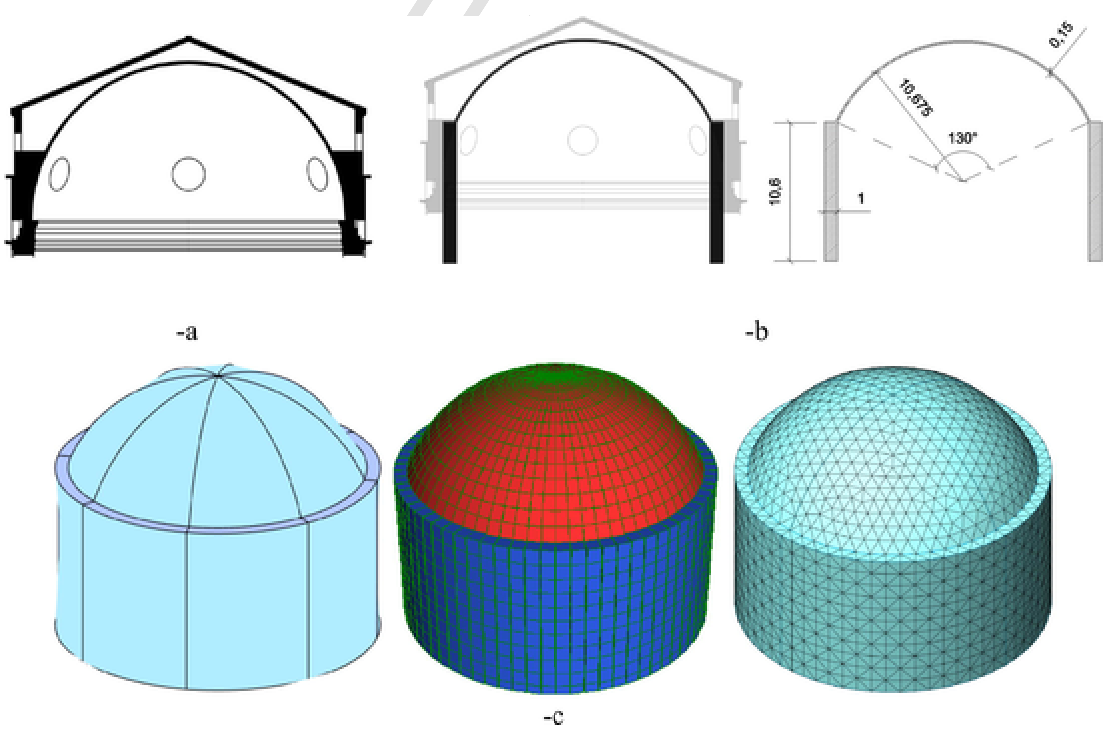

Fig. 4. Montepulciano Cathedral dome. –a: real geometry of the calotte and the drum. –b: idealized geometry studied in the paper. –c: models adopted (left: NURBS limit analysis discretization; center: FE discretization with brick elements; right: FE discretization with tetrahedrons.

Table 1
Montepulciano Cathedral dome. Masonry parameters adopted in the adaptive NURBS-limit analysis (for symbols meaning the reader is referred to Fig. 1).

Property	Symbol	Value	Unit of measure
Specific weight	γ	18	kN/m^3
Ultimate tensile strength	f_t	0–0.2	MPa
Cohesion	c	0.06	MPa
Friction angle	Φ	22	°
Ultimate compressive strength	f_c	2.4	MPa
Parameters defining the shape of the linearized compressive cap	ρ	0.5	–
	Φ_2	10	°

Table 2
Masonry parameters adopted for the FE pushover analyses. A Total Strain Based Crack model is used for masonry.

Property	Symbol	Value	Unit of measure
Young's modulus	E	1500	MPa
Poisson's coefficient	ν	0.2	–
Specific weight	γ	18	kN/m^3
Ultimate tensile strength	f_t	0.2	MPa
Ultimate tensile strain	ε_u	0.0001	–
Ultimate compressive strength	f_c	2.4	MPa
Shear retention factor	β	0.33	–

sults are quite sensitive to the value adopted for the tensile strength, a result that is not surprising, considering failure mechanisms obtained with the approach proposed and depicted in Fig. 6. As can be observed, the mechanism is formed by an annular flexural hinge near the top and meridian cracks, associated to velocity jumps along parallels. Dissipation is therefore exclusively ruled by f_t, and this justify the large variability of collapse loads obtained. In any case, when results are compared with those obtained through the non-linear FE model, two issues should be considered, namely that in the FE incremental model a much higher peak tensile strength is assumed (200 kPa against 40 kPa), but followed by a steep softening. In limit analysis, which assumes materials behaving in a perfect plastic way, it is therefore recommended to properly limit masonry strength in tension, or at least consider residual values (if any) instead of peak ones.

Another key issue is worth nothing, see Fig. 6, namely the dependence of the value of collapse load found on the number of fracture lines along meridians considered. As can be observed, it is recommended to subdivide with 10–12 meridians the NURBS mesh to obtain reliable results, a practical rule that obviously holds only for this particular case where the dissipation along meridians becomes crucial.

3.2. Half calotte under distributed vertical load

Often, after the collapse of a masonry dome, it is found that about one-half of the dome remains erect. Certainly, it is not possible to justify the stability of this structure under vertical loads considering a simple one-dimensional behavior, for example schematizing through independent curved cantilevers. However, it makes sense to analyze the static behavior of one-half of the calotte under – in addition to self-weight – the same vertical distributed load considered for the entire dome and increased up to the activation of the failure mechanism. It is intuitively evident that the expected structural behavior still remains 2D, but hooping meridian compression stresses, which help in increasing the load bearing capacity of the entire calotte, here should play a much less important role, because of the presence of free vertical edges. It is also expected that the collapse load strongly decrease.

In analogy with what done for the entire calotte, in Fig. 7 the global load-displacement curve obtained with the non-linear FE model is depicted for the semi-calotte. In addition, the collapse loads obtained with limit analyses at different values of masonry tensile strength are reported. Analyzing incremental FE results, it can be seen how the behavior is extremely fragile. Furthermore, comparing the damage distribution at peak (point A) and that at the last iteration in the softening region (point B), again reported in Fig. 7, it can be observed how the crack pattern does not provide a very clear information of the complex mechanism associated to failure. Limit analysis helps much more in this regard, showing (see Fig. 7) that the semi-calotte collapses for the formation of a network of very curved yield-lines (not easily reproducible with standard methods) working in bending, with a diagonal in-plane crack forming in the drum, which is clearly visible also in the FE incremental model. Let us finally observe that the semi-calotte and semi-drum system analyzed resembles closed to two famous Roman dome ruins that are still standing, namely those of the temple of Minerva Medica and those of the dome of the Baths of Caracalla.

3.3. Calotte subjected to horizontal force distributions simulating seismic actions

The main aim of the limit analysis model here presented is to provide a tool for the ultimate limit state analysis (i.e. prediction of col-

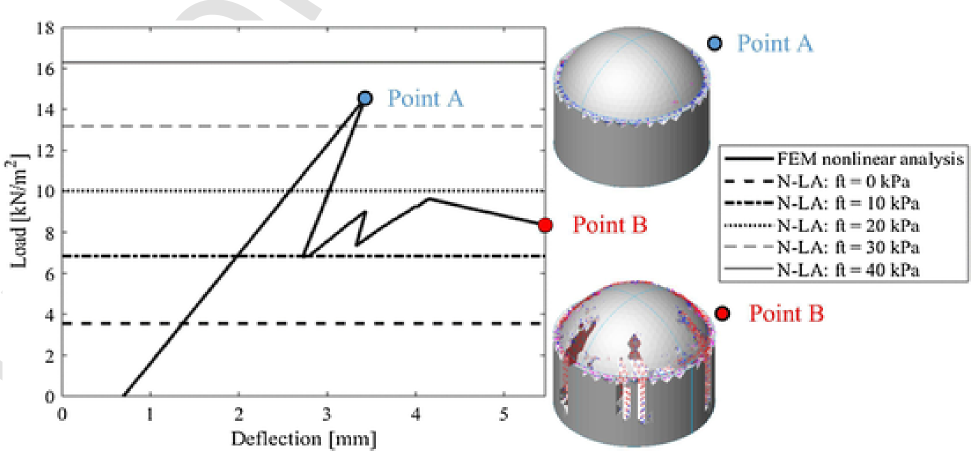

Fig. 5. Montepulciano Cathedral dome. Analyses under distributed vertical loads increased up to collapse, FE non-linear load deflection curve and limit analyses collapse loads varying masonry tensile strength.

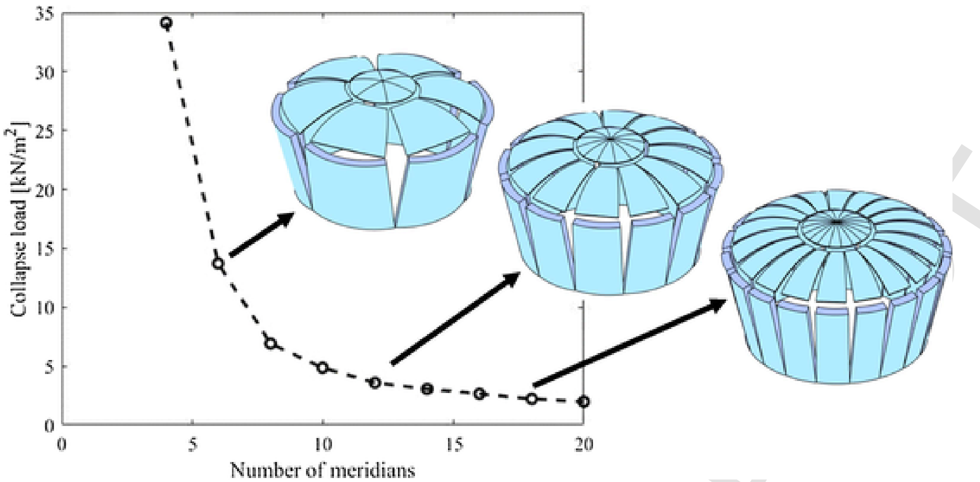

Fig. 6. Montepulciano Cathedral dome. Collapse load convergence study at progressively increased number of fracture lines along meridians with null value of tensile strength: collapse mechanism for 6 meridians, 12 meridians, 18 meridians and collapse multipliers obtained.

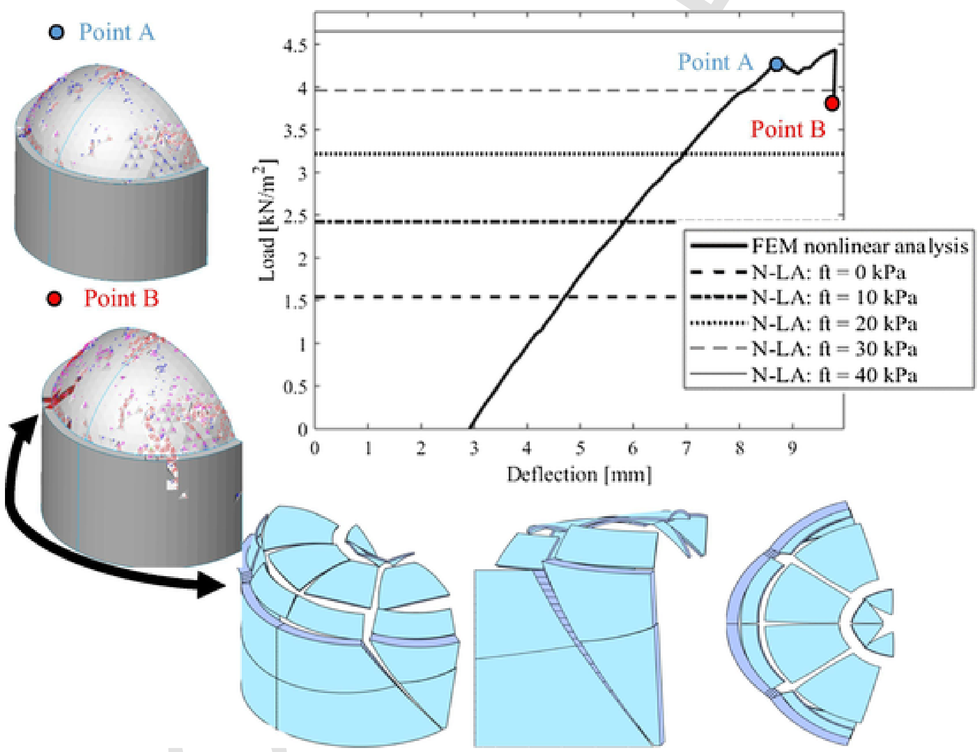

Fig. 7. Montepulciano Cathedral dome. Analyses under distributed vertical loads increased up to collapse, FE non-linear load deflection curve and limit analyses collapse loads varying masonry tensile strength.

lapse loads and active failure mechanisms) of masonry domes subjected to statically equivalent seismic loads.

As far as the distribution of horizontal loads to apply is concerned, the new Italian norms for constructions NTC2018 [55] recommend for masonry structures to apply incrementally a horizontal distribution of accelerations either proportional to the first mode of vibration (first type distribution, if the excited mass of the mode is >60%) or constant along height.

Fig. 8 shows the first modal shape as obtained through the symmetric FE discretization of Fig. 4. Values of normalized displacements are kept in the centroids of the elements for the sake of simplicity, and this justified the stepped resolution obtained with the thick continuous line. As it is possible to observe, the deformed shape can be well approximated by a linear distribution along the height and a cosine-shaped distribution in plan. To have at disposal an analytical representation of the applied horizontal forces depending on the load multiplier is particularly convenient for the NURBS approach here proposed, because the program through numerical integration carries out computations automatically. Taking into account this important practical aspect, limit analyses under horizontal loads are performed with the four different distributions of horizontal loads summarized in Fig. 9.

In Fig. 10, the load-displacement curve obtained by means of the FE nonlinear model is depicted with cracks patterns appearing in two meaningful instants, labeled as A and B. With the term load, it is intended the distributed pressure applied on the surface of the elements located in the upper edge of the calotte and as control node the apex of the dome is assumed. Point A is at peak, whereas B is located at the end of the simulation, where the failure mechanism is intended fully

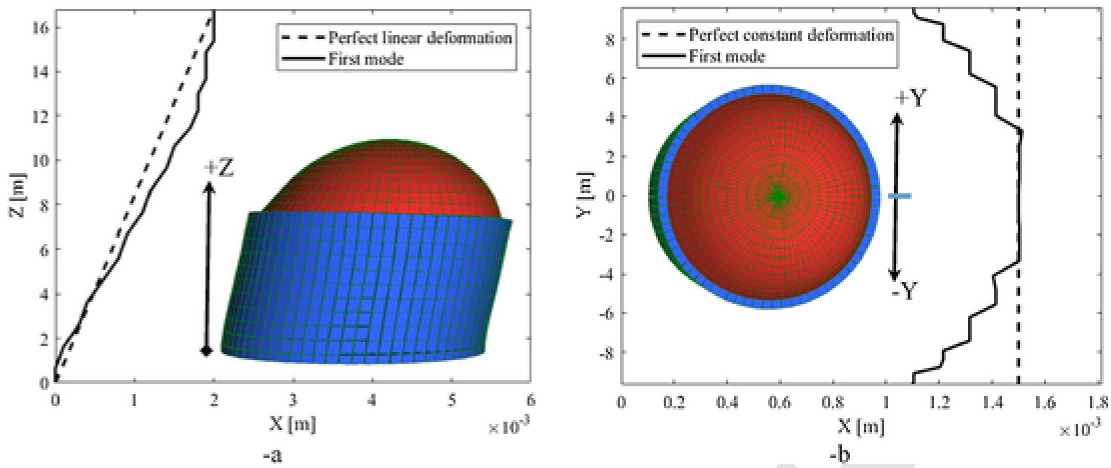

Fig. 8. Montepulciano Cathedral dome. Analysis of the first mode deformation. –a: deformation along the height; -b: deformation on the horizontal plan (at the dome's base).

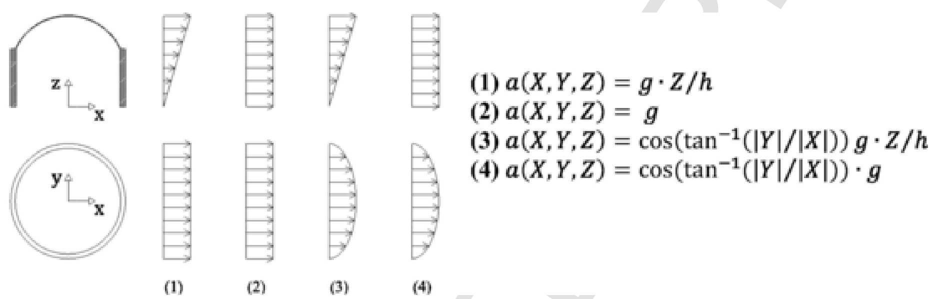

Fig. 9. Montepulciano Cathedral dome. Four configurations of accelerations applied.

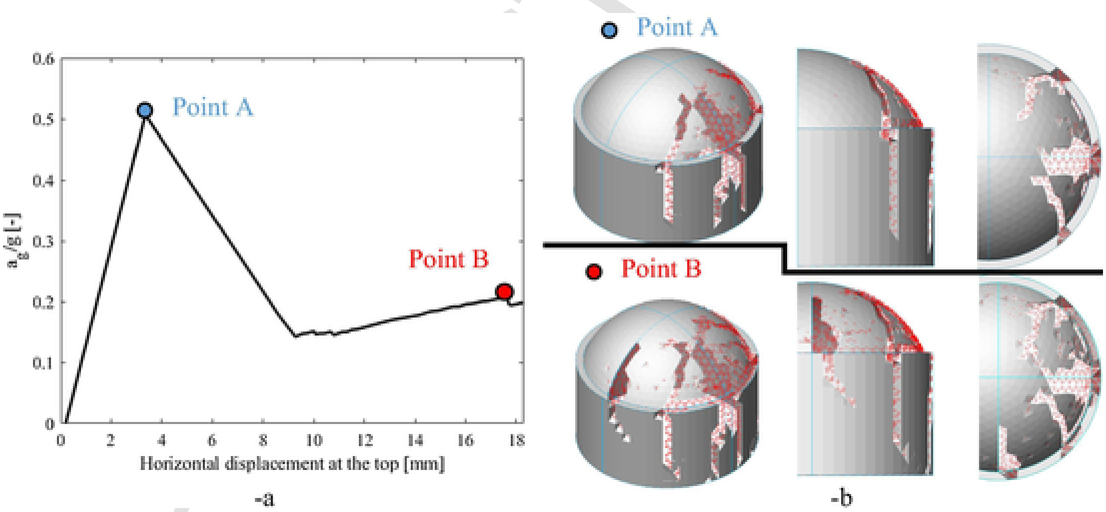

Fig. 10. Montepulciano Cathedral dome. -a: Nonlinear FE analysis under horizontal forces on the whole structure, type 1 distribution of loads (proportional to first mode deformed shape). –b: crack pattern at steps A & B (perspective, lateral and plan views).

developed and the structure is prone to collapse. As can be observed, softening is extremely steep in this case and cracks diffuse quickly after the peak load is reached, as demonstrated by the differences in the crack patterns obtained for points A and B. Fig. 10 shows also the failure mechanism found with the same distribution of horizontal loads with the NURBS approach, as well as the different collapse loads obtained progressively increasing masonry tensile strength. Analogously to what observed in the case of vertical loads increased up to failure, a very good prediction of the peak load is obtained assuming for masonry a tensile strength equal to 40 kPa, a value that is 1/5 of the peak strength adopted in the FE incremental analyses. Again, practical recommendations about the reduction of the expected masonry tensile strength could be given to practitioners in order to remain on the safe size and properly account for the fragile behavior of masonry in tension. In any case the no-tension material hypothesis is always very conservative and, hence, in reality and extra resistance of the structure is more likely.

An important aspect to underline is also the very good prediction by NURBS limit analysis of the crack pattern forming the failure mechanism, with the opening of a diagonal crack in the drum upper part, see Fig. 10. The diagonal cracks is visible at failure also in the FE incremental model, as well as the flexural hinge forming at the drum/calotte connection. In this regard, limit analysis failure mechanism is much more understandable and provides a more interesting insight into the behavior of the structure at collapse. The identification of such a clear collapse mechanism is also useful to perform non-linear static analyses which are much less demanding than those performed here, simply re-meshing the structure with elastic elements and non-linear interfaces where the yield lines are located.

The results obtained in terms total shear at the base at collapse considering the dome subjected to all four distributions of horizontal forces are finally reported in Table 3, whereas a comparison with the result of the nonlinear FE analysis is depicted in Fig. 11. Fig. 12 shows the collapse mechanisms obtained. A tensile strength equal to 200 kPa is adopted in this case, as in the FE incremental simulations. It is interesting to point out how the obtained total shear at the base is different from case to case, because the load distribution is different; on the contrary, collapse mechanisms are quite similar, see Fig. 12. This is not surprising, because despite the velocities fields at collapse are almost superimposable; power dissipated by external loads is different because of the different distribution of the forces applied. An interesting final qualitative aspect to point out is also that the still standing part after the collapse reproduces quite closely some situations of dome ruins nowadays visible in seismic zones, suggesting that one possible cause of collapse of ancient domes may be probably ascribed to strong earthquakes.

4. Collapse of the dome of the church of Anime Sante

The second benchmark considered to validate the NURBS approach here proposed is the dome of the Church of Anime Sante, destroyed on 6th April 2009 by L'Aquila earthquake (Mw = 6.3, ML = 5.8).

The construction of the Anime Sante Church begun in 1713 to commemorate the victims of the earthquake that destroyed the city of L'Aquila in 1703. The church consists of a rectangular hall with a barrel vault flanked by two chapels on each side, with eight windows placed to illuminate the presbytery from the hemispherical dome, Fig. 13. The design was entrusted to Carlo Buratti student of the famous baroque architect Carlo Fontana. The definitive completion of the church will be in 1805 with the realization of the dome attributed to Giuseppe Valadier and already conceived in the original project of the building written by the Buratti a century earlier. L'Aquila earthquake in 2009 caused 308 victims and seriously damaged the historical city center. The Anime Sante Church had the same destiny—the earthquake being responsible for the collapse of both the lantern and the dome, diffused cracks of the key stone arches, detachment of the facade and apse and shear cracking of several walls. The still standing parts of the drum and the dome are visible from photos reported Fig. 13, where the geometry of the drum/dome system is also shown by means of a transversal section.

In absence of specific data to assign to masonry mechanical properties, for the numerical simulations here reported, the same parameters adopted in the previous Section are assumed. In general, such data are in agreement with Italian code, more precisely with Explicative Notes [56] for existing buildings. Fig. 14 depicts the NURBS model of the system constituted by drum, dome and lantern in Rhinoceros and the MATLAB NURBS FE implementation used for the limit analyses.

The results obtained considering the dome subjected to all four distribution of horizontal forces discussed in the previous Section are reported in Table 4 and Fig. 15, whereas Fig. 16 shows the collapse mechanisms obtained in the different cases. Considerations similar to those done in the previous case can be repeated here. In particular, the failure mechanism does not change too much with the distribution of horizontal loads applied, conversely the collapse acceleration is very sensitive to the actual distribution of accelerations. In agreement with consolidated literature in the field and with the Italian code, the most conservative case is an inverse linear distribution along the height with cosine variability in plan, i.e. which follows the first mode.

Table 3
Results obtained for each distribution of horizontal acceleration.

Configuration of accelerations #	Corresponding base shear [kN]	a_g/g [−]
(1)	3470	0.260
(2)	5327	0.401
(3)	2884	0.171
(4)	4086	0.307

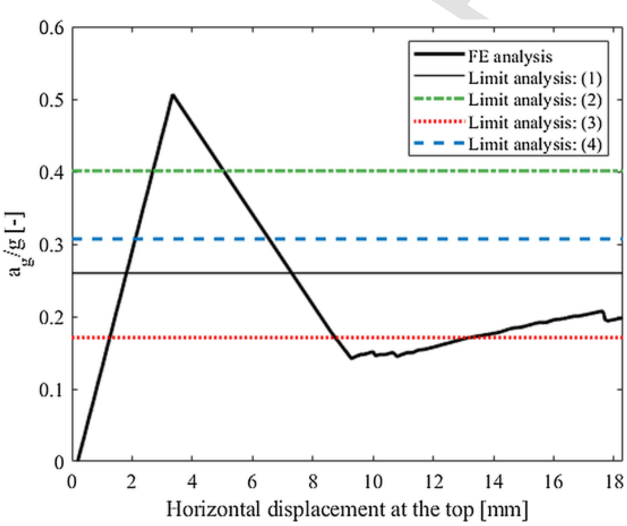

Fig. 11. Results obtained for each distribution of horizontal acceleration.

5. "Calidarium" of the Baths of Caracalla

The last example discussed is the limit analysis under horizontal loads of the Calidarium of the Baths of Caracalla. The Baths of Caracalla are a monumental complex located in Rome city center (near Colosseo), built in Roman age (212–216 A.C.), and conceived as imperial public baths (thermae) for wealthy people. Calidarium was a room with a hot plunge bath, used in Roman bath complexes, in this case almost isolated from the rest, with circular plan and covered by a dome, hence with a typical shape that can be studied with the present approach, see Fig. 17.

In 537 during the Gothic War, Vitiges king of the Ostrogoths laid siege to Rome and severed the city's water supply. Shortly thereafter, the baths were abandoned. Located too far away from the still populated area of Rome, the baths were mostly disused.

According to [57], the earthquake of 847 destroyed much of the building, including Calidarium along with many other Roman structures. This Section is aimed at discovering if the NURBS limit analysis approach proposed is able to (a) predict a failure mechanism which justifies the actual situation of the still standing ruins and (b) provide a collapse acceleration compatible with a moderate/strong PGA occurred in the past in Rome.

The real shape of the Calidarium and the correct dimensions of its architectural elements are not known with absolute certainty, but currently only some reconstructions are available. DeLaine's book on the Baths of Caracalla [57] is the only published collection of detailed geometrical and constructive information for the site. The DeLaine's geometrical reconstruction is shown in Fig. 17. However, there are many others different interpretations: an example is Palladio, which represents the Calidarium characterized by a geometry very similar to that of the Pantheon and with some differences compared to the work of

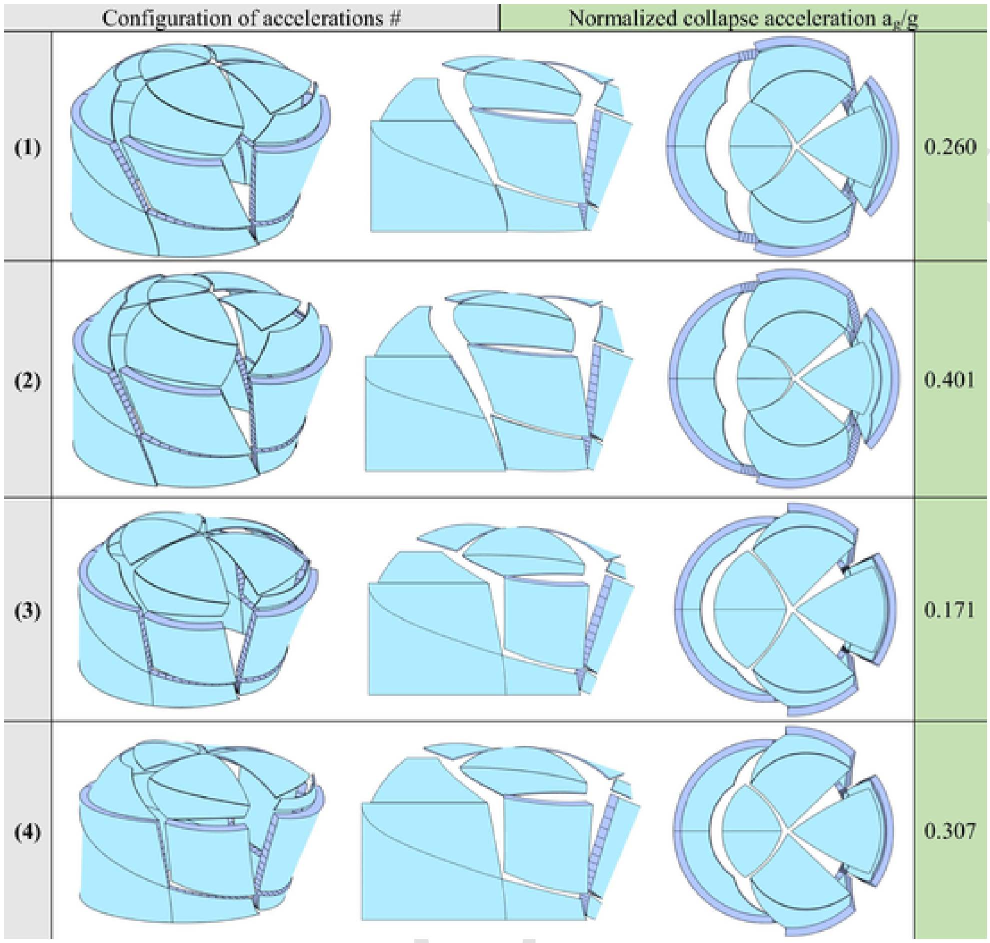

Fig. 12. Montepulciano Cathedral dome. Collapse mechanisms obtained for the four load configurations considered (perspective, lateral and plan views).

DeLaine (such as the presence of an oculus at the top of the dome and as the different height of openings).

According to such researches, the plan view shows a structure composed by an internal diameter of 36 m and pillars with a thickness of 6 m (equal to 1/6 of the external radius). Another thickness of 2.7 m, over which the columns are based is added, in this way an external diameter of 53.4 m is obtained. Column diameters are equal to 3 feet (0.9 m) and the interspacing is three times wider, in agreement with Vitruvius recommendations. Two levels of vaults can be observed from the cross sections. The first one consists in vaults with springing located at a height of 11 m from the ground; conversely, those at the upper level have a particular shape which maximizes the light entering the structure. The thickness of the dome at the crown is equal to 1.5 m, as in the dome of the Pantheon.

As in many other roman buildings, the walls of the Baths of Caracalla had a composite structure made of two external brick walls with a triangular shape disposed as indicated in Fig. 18 and a concrete core. The inner nucleus was a conglomerate composed by pozzolanic lime mortar containing large pieces of stones marbles, tuff and bricks (opus caementicium). Considering the most common walls delimited by triangular bricks and obtained by diagonally cutting square bricks (typically 20 × 20 cm) the real bearing width of the masonry was only 7 cm, i.e. absolutely negligible when referred to walls with a thickness of some meters. Therefore, the mechanical characteristics of the wall depended almost exclusively on the resistance of the opus caementicium, which is much better than masonry used in the Middle Age. In this regard, the present example is very different with respect to the previous ones and the adoption of a no-tension material model is not suitable in this case.

Therefore, for the evaluation of the structural behavior of a roman building, an accurate knowledge of the mechanical characteristics of the opus caementicium is essential. The distribution of materials in the Calidarium has been modeled reproducing the stratigraphy observed in the semi-dome of the exedra of the West palestra, in which different types of caementa are arranged in a descending order of specific weight (see Fig. 17). They contain as main component: bricks, tuff and Vesuvian scoria. Columns, arranged inside the vaults of the first level, were made of travertine marble.

In the following analyses, the dome has been considered as isolated from other structures, a hypothesis which appears reasonable considering the plan distribution of the different parts, Fig. 17.

A representation by NURBS surfaces of the Calidarium has been obtained –analogously to the previous cases- through the software Rhinoceros. By importing the geometry in MATLAB and assigning "thickness" and "offset" properties to each surface, the NURBS model adopted for the presented adaptive limit analysis has been obtained, see Fig. 19. Some approximations have been necessarily applied on the geometrical model, because the presented procedure does not allow to reproduce vaults with variable thickness. Therefore, an average thickness value has been assigned to the dome and openings have been regularized by applying the same "opened-area" inside and outside of the tambour. Moreover, marble columns have not been taken into account in this model. A total number of 37 surfaces have been adopted for the initial NURBS model. The initial model is shown in Fig. 19. The initial number of surfaces used is relatively large because of the need to represent correctly arches and assign different specific weight values. Mater-

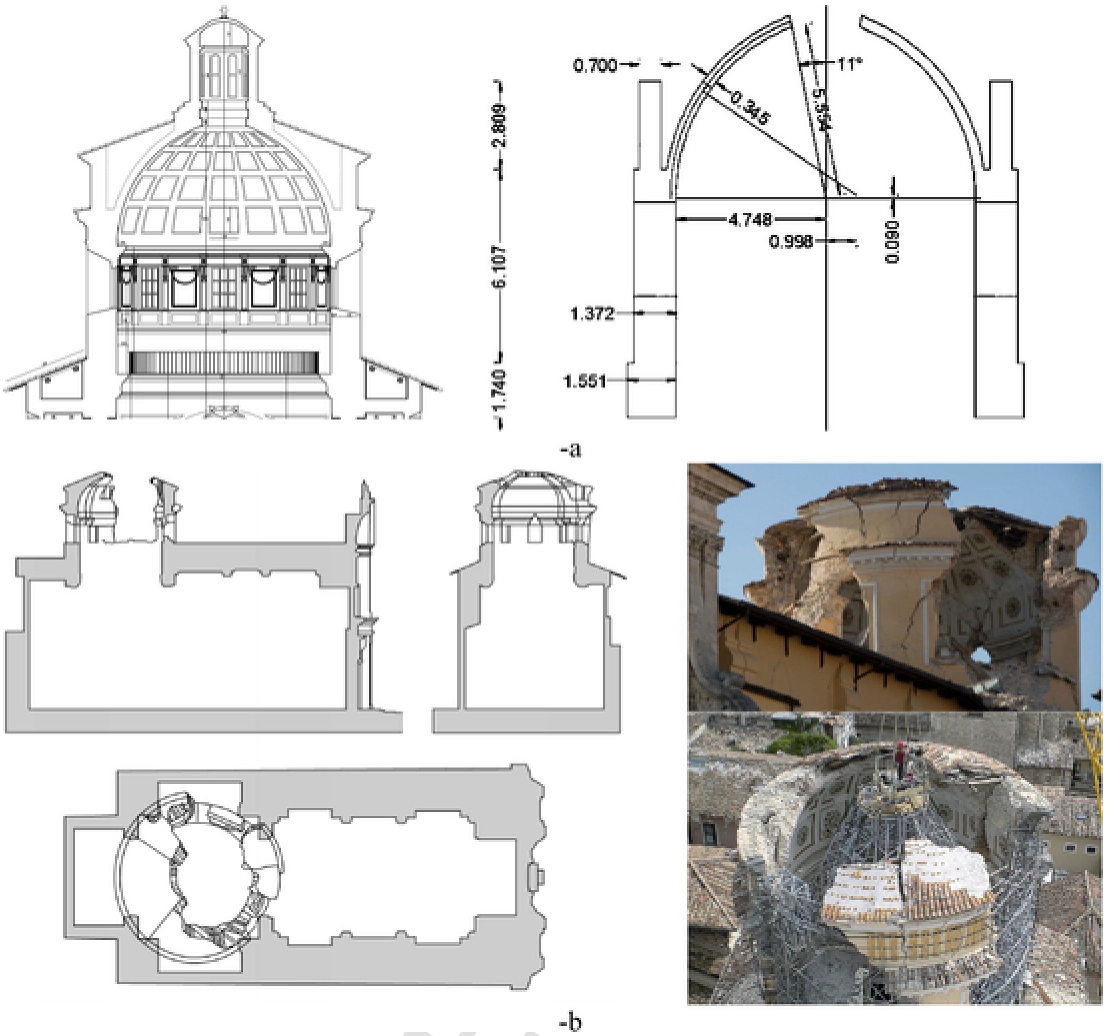

Fig. 13. Dome of Anime Sante Church. –a: geometry before the earthquake; -b: still standing parts after the collapse.

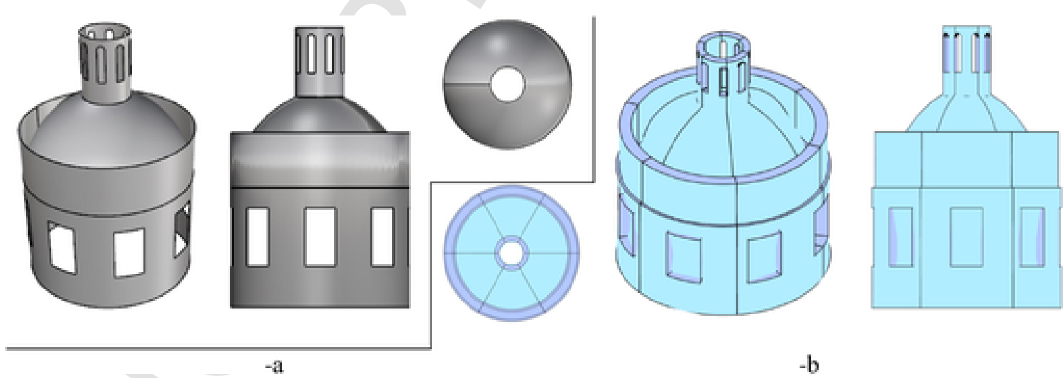

Fig. 14. Dome of Anime Sante Church. NURBS model in Rhinoceros (-a) and after NURB discretization in Matlab (-b).

ial properties adopted for Roman concrete in limit analysis are reported in Table 5.

The same four configurations of horizontal accelerations used in the previous benchmarks are applied also in this case and results (failure mechanisms and normalized accelerations at failure) are summarized in Fig. 20. The collapse mechanism is very similar in all cases; differently to the case of Anime Sante, in this case the entire dome collapses. This can be due to the presence of a tambour characterized by many openings, which makes the upper part less stable against horizontal loads. The dome seems to collapse for the formation of a complex yield pattern but also for a rigid sliding over the pillars of the second level, which suffer for overturning. The fracture lines in the dome, clearly visible along meridians directions, are connected with the vertical fracture lines in the tambour.

In order to validate quantitatively the limit analysis approach adopted, a nonlinear static analysis (pushover) is performed on the same 3D geometric model considered for limit analysis computations. A FE mesh with around 53,000 tetrahedron elements is utilized, as shown Fig. 19. Elastic and inelastic properties of the Roman concrete in the three levels are collected in Table 6.

Table 4
Dome of Anime Sante Church. Results obtained for each distribution of horizontal acceleration.

Configuration of accelerations #	Corresponding base shear [kN]	a_g/g [−]
(1)	1520	0.237
(2)	2296	0.354
(3)	1405	0.217
(4)	2104	0.325

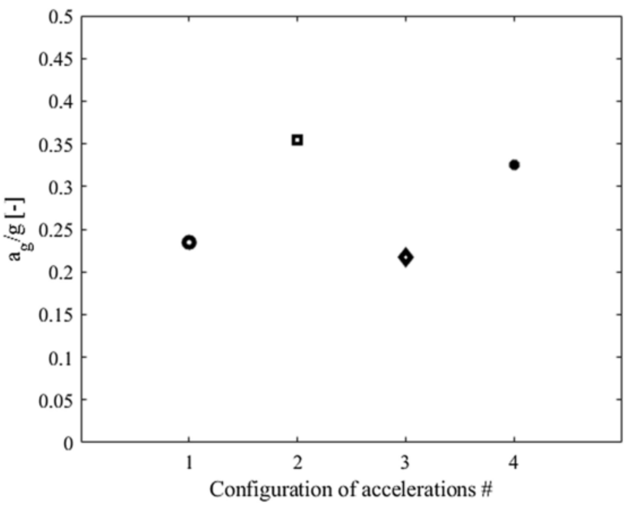

Fig. 15. Dome of Anime Sante Church. Results obtained for each distribution of horizontal acceleration.

All the different types of Roman concrete are assumed with the same compressive strength of 5 MPa and with a tensile strength equal to one-tenth of the compressive one, in agreement with some experimental data available for coeval structures in the same region. The non-linear behavior of the Roman concrete is reproduced numerically by mean of a Concrete Damaged Plasticity material model already available in the software used [58].

The definition of the post peak tensile response does not reference to any experimental data, as, unfortunately, no post-peak results have been yet published. However, a bilinear softening law was determined by [59] from a series of experimental arc-shaped three-point bending tests on recreated Roman pozzolanic mortar samples. To evaluate the material response in post-critical range, a displacement controlled bending procedure (CMOD or crack width measure) was developed such that a load-point displacement was applied at the top of the arc samples while two rollers supported the base. The interested reader is referred to [59] for further details. According to experimental data, the bilinear curve depicted in Fig. 21 with values as in Table 6 is adopted in the FE non-linear model.

A comparison between pushover curve obtained with the non-linear FE model and limit analysis prediction (horizontal load distribution #(3)) is reported in Fig. 22, with deformed shapes and developed cracks provided by the two models (left: FE non-linear analysis and damage patch in tension; right: NURBS limit analysis active failure mechanism). Two main aspects are worth noting from a detailed analysis of the results obtained, namely (1) the very good agreement in terms of deformed shapes at collapse and crack pattern distributions provided by the two numerical models and (2) the values of acceleration at collapse obtained, again very close one each other.

The agreement of deformed shapes, crack patterns and failure accelerations found suggests that the NURBS procedure proposed is a very effective tool that is not only predictive of the actual behavior of such kind of structures under horizontal loads, but that should be preferred non-linear FE computations carried out with refined meshes and softening materials. Typically, this latter approach is computationally very demanding, the obtained results turn out to be dependent on a series of non-linear material parameters difficult to determine and requires very experienced users and a convenient theoretical background. On the contrary, the limit analysis approach proposed is immediate, does not require any expertise by the user (exception made that a general knowledge of a Cad software) and furnishes very clear mechanisms that can be used also in advanced non-linear computations with concentrated non-linearity.

As far as the collapse acceleration found is concerned, it should be finally pointed out that the value numerically estimated could be compatible with a PGA of a strong earthquake occurred in the past in Rome. For instance, there is memory of a ‘big one’ earthquake occurred near Rome presumably of magnitude 7 or more in 1915, with epicenter near the town of Avezzano 100 km east of Rome, which caused damage to buildings and Roman monuments in Rome. Probably many moderate/strong earthquakes took place from Gothic war to the renaissance period, with unknown PGAs but probably compatible with the collapse of the structure. In addition, the still standing ruins configuration is very similar to that predicted by limit analysis. Another aspect worthy of investigation could be the cumulated damage caused by the application of repeated accelerograms. This latter issue is however reproducible numerically only with non-linear dynamic analyses.

6. Conclusions

Recent strong earthquakes occurred in Italy (Umbria-Marche 1997–98, L’Aquila 2009, Emilia 2012 and Central Italy 2016) caused serious damages and collapses to the architectural historical heritage and in particular to several masonry domes. This shows the high vulnerability of such kind of structures, but at the same time, the need to make available computational tools to predict the accelerations associated to the activation of a failure mechanism and the mechanism itself, this latter information being paramount for an effective local strengthening. The present paper aims at presenting a fast and reliable automatized kinematic limit analysis approach able to accurately predict the actual behavior of masonry domes subjected to horizontal static seismic loads. The model uses a rough discretization of the dome obtained by means of few rigid-infinitely resistant NURBS generated elements, adapting step by step the initial mesh in order to progressively overlap the element edges (where all dissipation is lumped) with the hinges forming the failure mechanism. The adoption of a rough mesh makes the code extremely fast, much more competitive than a standard FE model, allowing at the same time to approximate the actual geometry and load distributions in an extremely accurate way. The utilization of geometries obtained with laser scanner acquisitions is straightforward and the presence of pre-existing cracks can be accounted for as well. Three complex actual historical masonry belonging to the Italian cultural heritage domes are analyzed in detail to benchmark the approach proposed. The first example has the geometrical parameters of a typical late Renaissance dome, the dome of Montepulciano cathedral. The second is the dome of the eighteen-century church of Anime Sante (collapsed during the L’Aquila 2009 earthquake with a paradigmatic failure mechanism). The last is the dome of the Calidarium of the Baths of Caracalla built in the second century after Christ, whose causes of collapse remain unknown. All simulations performed show the reliability of the simple adaptive approach proposed by the Authors able to quickly provide collapse accelerations and failure mechanisms. Therefore, it appears convenient to adopt such a kinematic approach to deal with the limit analysis of domes subjected to horizontal loads, instead of pursuing strategies based on the thrust network analysis or direct FE computations, which require experience users and potentially long time to be performed. The adopted NURBS representation has proven to be

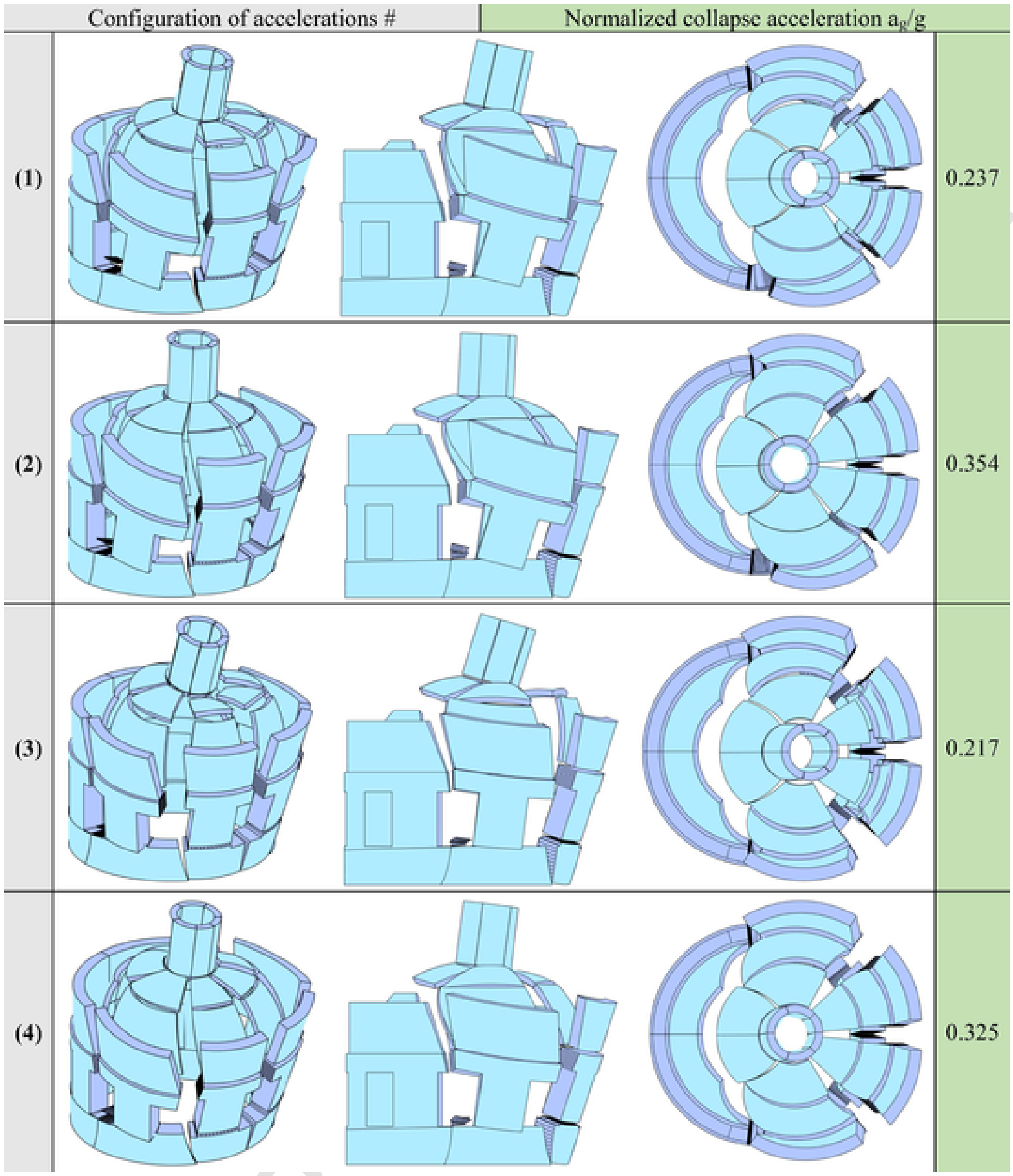

Fig. 16. Dome of Anime Sante Church. Collapse mechanisms obtained for the four configurations of acceleration considered (perspective, lateral and plan views).

particularly suited for the limit analysis of curved geometries from a three-dimensional point of view. However, it has to be mentioned that this method is actually limited to structures which are representable through an assemble of surfaces. In some cases, such as masonry structures described by variable or not negligible thickness values in comparison with other dimension (as for the Calidarium of Caracalla), simplifications in the initial geometries or in the structural behavior are necessarily required. Therefore, future research will address the development of new efficient modeling strategies based on NURBS volumes instead of surfaces. In this way, the field of application will be extended to more complex structures, such as towers, masonry arches interacting with the infill, and vaults with variable thickness values.

Acknowledgements

A. Tralli wishes to thank Prof. M. Como for discussions on the collapse of masonry domes subject to earthquakes

Appendix A. Supplementary material

Supplementary data to this article can be found online at https://doi.org/10.1016/j.engstruct.2019.109517.

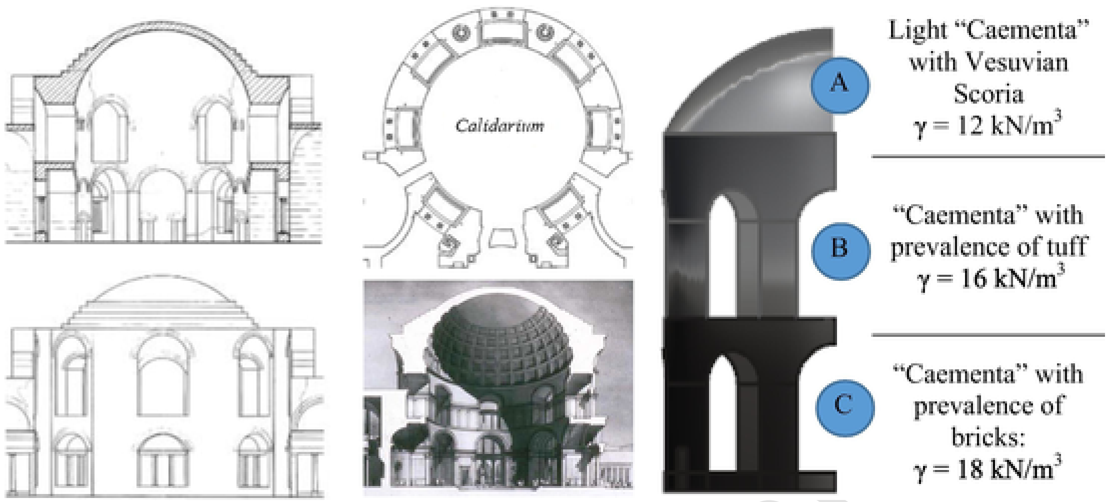

Fig. 17. Caracalla Calidarium. Reconstruction, cross section, lateral view and plan view, drawing by Palladio and weights of the different parts.

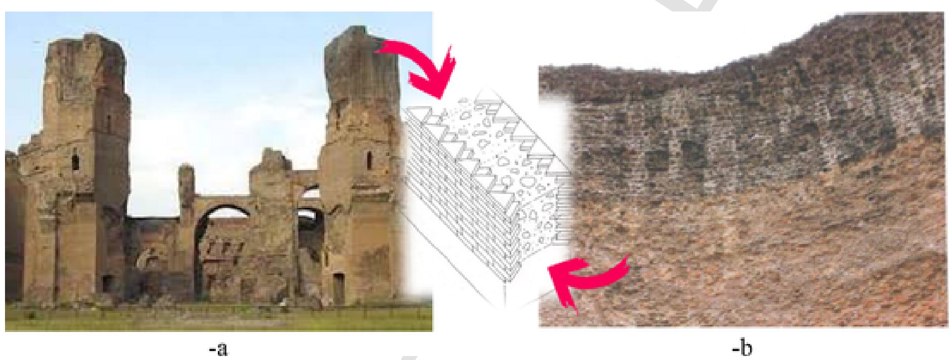

Fig. 18. Caracalla Calidarium. Still standing ruins composed by opus caementicium contained within two facing walls of triangular bricks (-a), view of different types of caementa (-b).

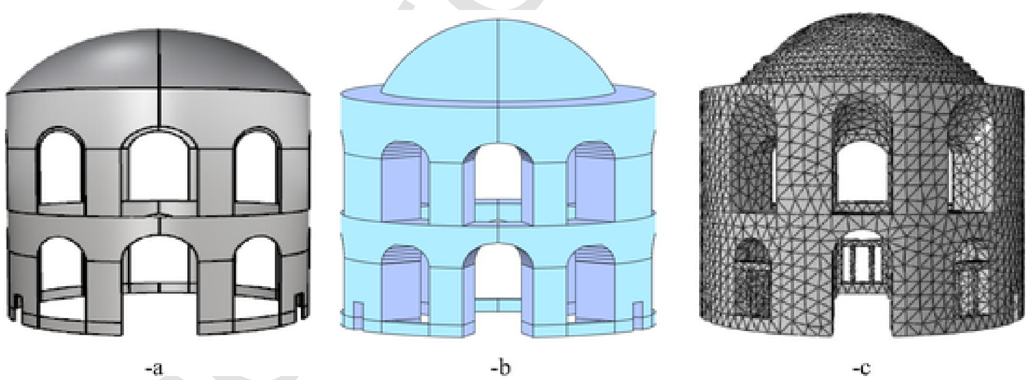

Fig. 19. Caracalla Calidarium. –a: NURBS model in Rhinoceros; -b: NURBS model in MATLAB and –c: 3D FE non-linear model (tetrahedron elements).

Table 5
Caracalla Calidarium. Material properties adopted for the NURBS limit analyses.

Specific weight	γ	12-16-18	kN/m^3
Tensile strength	f_t	0.25	MPa
Compressive strength	f_c	5	MPa
Cohesion	c	0.5	MPa
Friction angle	φ	22	°
Linear cap in compression	ρ	0.5	–
	φ_2	10	°

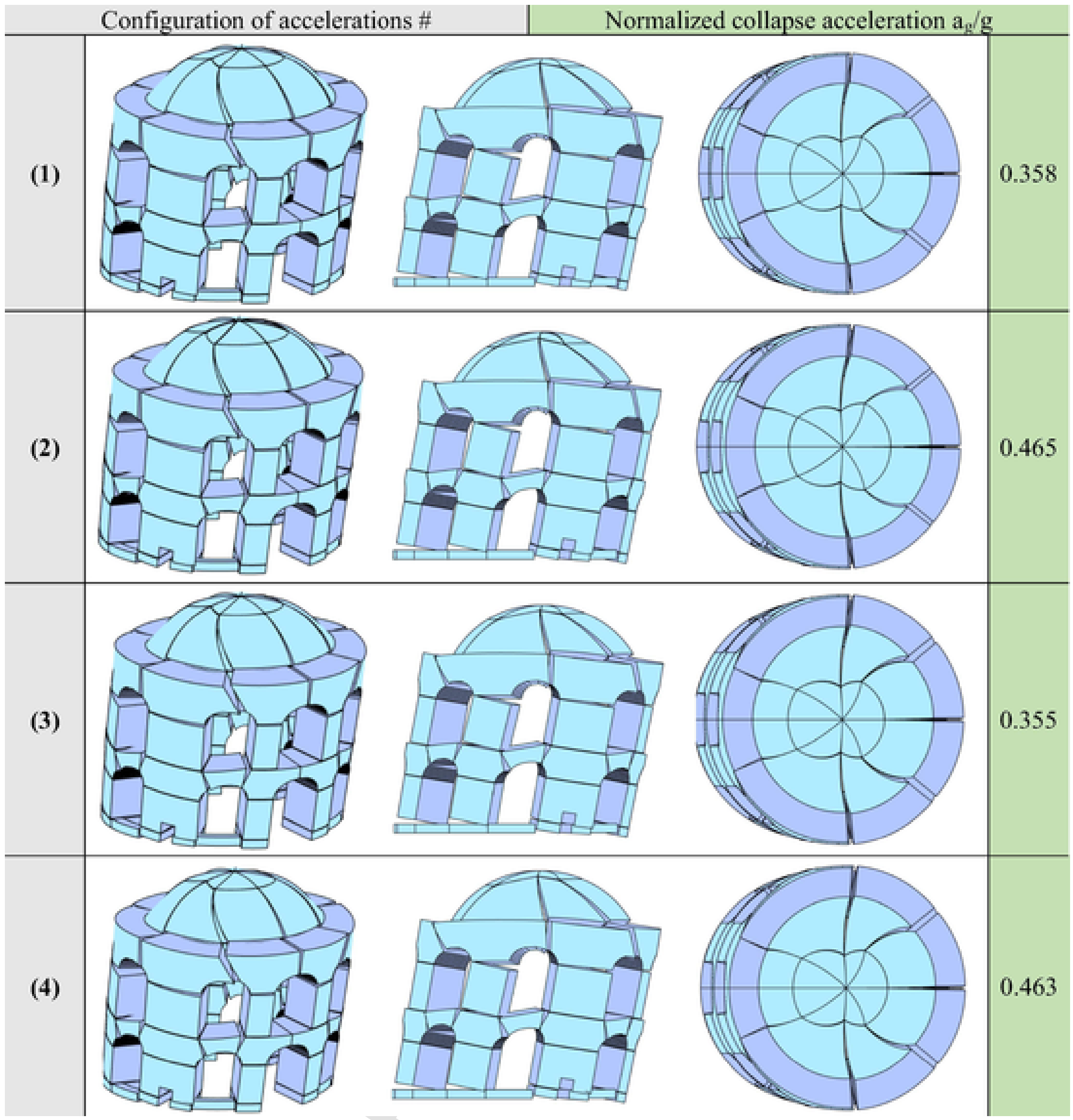

Fig. 20. Caracalla Calidarium. Results of the NURBS limit analyses (collapse mechanisms shown in axonometric view, perspective and horizontal view).

Table 6
Caracalla Calidarium. Elastic and inelastic (tensile behavior) properties assumed for the Roman concrete.

Density ρ [kg/m³]	Elastic modulus E [GPa]	Poisson's ratio ν [–]	Fracture energy G_f [J/m^2]	Tensile strength (yielding) f_t [MPa]	Tensile strength (intermediate) f_1 [MPa]	Intermediate CMOD value??$_1$ [mm]
1200/1600/1800	3.37	0.2	55	0.5	0.175	0.066

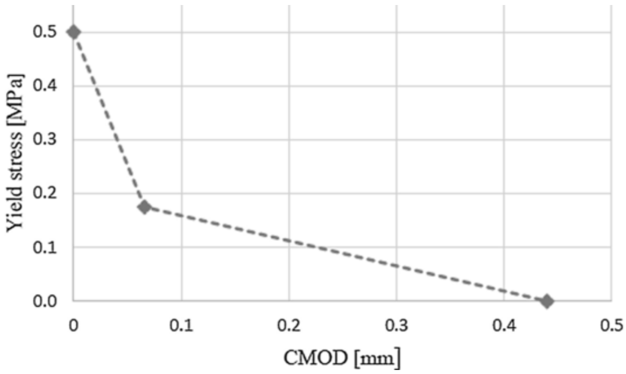

Fig. 21. Caracalla Calidarium. Bilinear tensile curve assumed in the post-elastic phase.

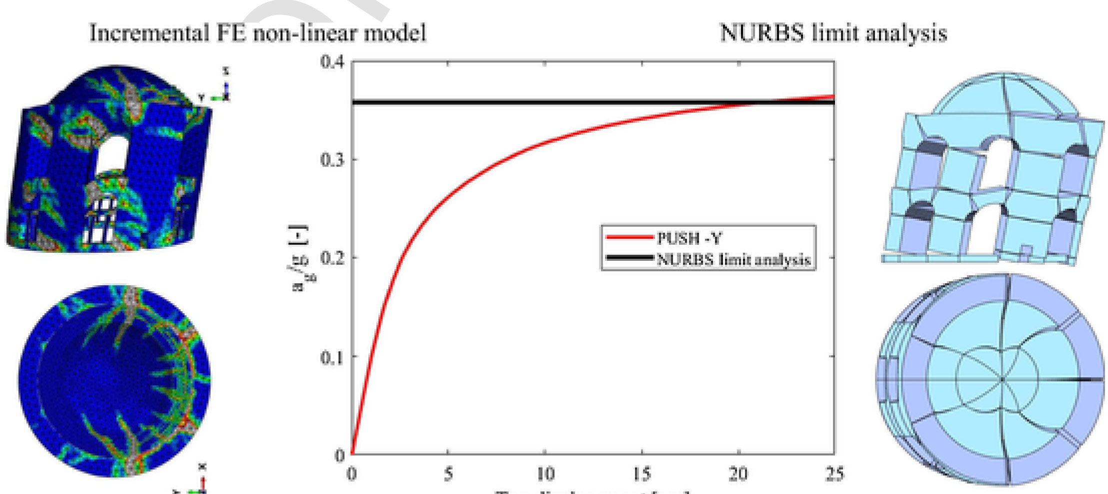

Fig. 22. Caracalla Calidarium. Comparison between pushover curve obtained with the FE non-linear model and collapse load provided by NURBS limit analysis.

References

[1] E Bertolesi, JM Adam, P Rinaudo, PA Calderón. Research and practice on masonry cross vaults – A review. Eng Struct 2019;180:67–88. doi:10.1016/j.engstruct.2018.10.085.
[2] Tralli A, Alessandri C, Milani G. Computational Methods for Masonry Vaults: A Review of Recent Results n.d.
[3] Heyman J. The Masonry Arch. Horwood; 1982.
[4] M Como. Statics of historic masonry constructions. Statics Hist Mason Constr 2013.
[5] M Pavlovic, E Reccia, A Cecchi. A procedure to investigate the collapse behavior of masonry domes: some meaningful cases. Int J Archit Herit 2016;10:67–83. doi:10.1080/15583058.2014.951797.
[6] J Heyman. The stone skeleton. Int J Solids Struct 1966;2:249–279. doi:10.1016/0020-7683(66)90018-7.
[7] J Heyman. On shell solutions for masonry domes. Int J Solids Struct 1967;3:227–241. doi:10.1016/0020-7683(67)90072-8.
[8] J Heyman. Equilibrium of shell structures. Clarendon Press; 1977.
[9] Benvenuto E. The history of strength of materials. Edizioni di Storia e Letteratura; 1981 [in italian].
[10] Beltrami E. On equilibrium of flexible and inextensible surfaces. Mem Dell'Accademia Delle Sci Dell'Istituto Di Bol 1882 [in Italian].
[11] W Flügge. Stresses in shells. Berlin Heidelberg: Springer-Verlag; 1962.
[12] A Kooharian. Limit analysis of voussoir (segmental) and concrete archs. ACI J Proc 1952;49. doi:10.14359/11822.
[13] J Heyman. The safety of masonry arches. Int J Mech Sci 1969;11:363–385. doi:10.1016/0020-7403(69)90070-8.
[14] S Huerta. The analysis of masonry architecture: a historical approach. Archit Sci Rev 2011.
[15] M Como. Statics of historic masonry constructions, 1. Berlin, Heidelberg: Springer Berlin Heidelberg; 2013.
[16] D O'Dwyer. Funicular analysis of masonry vaults. Comput Struct 1999;73:187–197. doi:10.1016/S0045-7949(98)00279-X.
[17] P Block, T Ciblac, J Ochsendorf. Real-time limit analysis of vaulted masonry buildings. Comput Struct 2006;84:1841–1852. doi:10.1016/j.compstruc.2006.08.002.
[18] P Block, J Ochsendorf. Thrust network analysis: A new methodology for three-dimensional equilibrium. J-Int Assoc Shell Spat Struct 2007;155:167.
[19] F Marmo, D Masi, L Rosati. Thrust network analysis of masonry helical staircases. Int J Archit Herit 2018;12:828–848. doi:10.1080/15583058.2017.1419313.
[20] F Fraternali. A thrust network approach to the equilibrium problem of unreinforced masonry vaults via polyhedral stress functions. Mech Res Commun 2010;37:198–204. doi:10.1016/J.MECHRESCOM.2009.12.010.
[21] M Angelillo, E Babilio, A Fortunato. Singular stress fields for masonry-like vaults. Contin Mech Thermodyn 2012;25:423–441. doi:10.1007/s00161-012-0270-9.
[22] A Chiozzi, G Milani, A Tralli. A Genetic Algorithm NURBS-based new approach for fast kinematic limit analysis of masonry vaults. Comput Struct 2017;182. doi:10.1016/j.compstruc.2016.11.003.
[23] LM Rios, NV Sahinidis. Derivative-free optimization: a review of algorithms and comparison of software implementations. J Glob Optim 2013;56:1247–1293. doi:10.1007/s10898-012-9951-y.
[24] E Milani, G Milani, A Tralli. Limit analysis of masonry vaults by means of curved shell finite elements and homogenization. Int J Solids Struct 2008;45:5258–5288. doi:10.1016/j.ijsolstr.2008.05.019.
[25] G Milani. Simple lower bound limit analysis homogenization model for in- and out-of-plane loaded masonry walls. Constr Build Mater 2011;25:4426–4443. doi:10.1016/j.conbuildmat.2011.01.012.
[26] G Milani. Upper bound sequential linear programming mesh adaptation scheme for collapse analysis of masonry vaults. Adv Eng Softw 2015;79:91–110. doi:10.1016/j.advengsoft.2014.09.004.
[27] G Lengyel. Discrete element analysis of gothic masonry vaults for self-weight and horizontal support displacement. Eng Struct 2017;148:195–209.
[28] V Sarhosis, K Bagi, JV Lemos, G Milani. Computational modeling of masonry structures using the discrete element method. IGI Global 2016.
[29] Clemente P, Raithel A. The mechanism model in the seismic check of stone arches. In: Sinopoli A, editor. Arch Bridg. Hist. Anal. assessment, Maint. repair, Rotterdam: Balkema; 1998.
[30] L De Lorenzis, M DeJong, J Ochsendorf. Failure of masonry arches under impulse base motion. Earthq Eng Struct Dyn 2007;36:2119–2136. doi:10.1002/eqe.719.
[31] M Rota, A Pecker, D Bolognini, R Pinho. A methodology for seismic vulnerability of masonry arch bridge walls. J Earthq Eng 2005;9:331–353. doi:10.1142/S1363246905002432.
[32] Resemini S, Lagomarsino S. Seismic Vulnerability of Masonry Arch Bridges. In: Proc 11th Ital Conf Earthq Eng, Genoa: 2004.
[33] P Zampieri, G Tecchio, F da Porto, C Modena. Limit analysis of transverse seismic capacity of multi-span masonry arch bridges. Bull Earthq Eng 2015;13:1557–1579. doi:10.1007/s10518-014-9664-3.
[34] C Pesciullesi, M Rapallini, A Tralli, A Cianchi. Optimal spherical masonry domes of uniform strength. J Struct Eng 1997;123:203–209. doi:10.1061/(ASCE)0733-9445(1997) 123:2(203).
[35] Homogenised limit analysis of masonry walls, Part I: Failure surfaces. Comput Struct 2006;84:166–80. http://doi.org/10.1016/J.COMPSTRUC.2005.09.005.
[36] G Milani, A Taliercio. In-plane failure surfaces for masonry with joints of finite thickness estimated by a Method of Cells-type approach. Comput Struct 2015;150:34–51. doi:10.1016/j.compstruc.2014.12.007.
[37] G Del Piero. Limit analysis and no-tension materials. Int J Plast 1998;14:259–271. doi:10.1016/S0749-6419(97)00055-7.
[38] Radenkovic. Théorèmes limites pour un materiau de Coulomb a dilatation non standardise. Comptes Rendue Académie Sci Paris 1961;252:4103–4104.
[39] J Salençon. Application of the theory of plasticity in soil mechanics. (USA): John Wiley & Sons; 1977.
[40] RK Livesley. Limit analysis of structures formed from rigid blocks. Int J Numer Methods Eng 1978;12:1853–1871. doi:10.1002/nme.1620121207.
[41] A Orduña, PB Lourenço. Three-dimensional limit analysis of rigid blocks assemblages. Part I: Torsion failure on frictional interfaces and limit analysis formulation. Int J Solids Struct 2005;42:5140–5160. doi:10.1016/j.ijsolstr.2005.02.010.
[42] S Tangaramvong, F Tin-Loi. Collapse load evaluation of structures with frictional contact supports under combined stresses. Comput Struct 2011;89:1050–1058. doi:10.1016/J.COMPSTRUC.2010.12.015.
[43] D'Ayala D, Casapulla C. Limit state analysis of hemispherical domes with finite friction. In: Lourenço PB, Roca P, editors. Hist Constr ons, Guimarães: 2001, p. 617–26.
[44] DF D'Ayala, E Tomasoni. Three-dimensional analysis of masonry vaults using limit state analysis with finite friction. Int J Archit Herit 2011;5:140–171. doi:10.1080/15583050903367595.
[45] L Schueremans, B Van Genechten. The use of 3D-laser scanning in assessing the safety of masonry vaults—A case study on the church of Saint-Jacobs. Opt Lasers Eng 2009;47:329–335. doi:10.1016/J.OPTLASENG.2008.06.009.
[46] AM D'Altri, G Milani, S de Miranda, G Castellazzi, V Sarhosis. Stability analysis of leaning historic masonry structures. Autom Constr 2018;92:199–213. doi:10.1016/J.AUTCON.2018.04.003.
[47] McNeel R. Rhinoceros: Nurbs Modeling for Windows. Robert McNeel & Associates; 2008.
[48] A Chiozzi, G Milani, A Tralli. Fast kinematic limit analysis of FRP-reinforced masonry vaults. I: General genetic algorithm-NURBS-based formulation. J Eng Mech 2017;143. doi:10.1061/(ASCE)EM.1943-7889.0001267.
[49] A Chiozzi, G Milani, A Tralli. Fast kinematic limit analysis of FRP-reinforced masonry vaults. II: numerical simulations. J Eng Mech 2017;143. doi:10.1061/(ASCE)EM.1943-7889.0001268.
[50] A Chiozzi, G Milani, N Grillanda, A Tralli. A fast and general upper-bound limit analysis approach for out-of-plane loaded masonry walls. Meccanica 2017. doi:10.1007/s11012-017-0637-x.

[51] A Chiozzi, N Grillanda, G Milani, A Tralli. UB-ALMANAC: An adaptive limit analysis NURBS-based program for the automatic assessment of partial failure mechanisms in masonry churches. Eng Fail Anal 2018;85. doi:10.1016/j.engfailanal.2017.11.013.
[52] JA Cottrell, TJR Hughes, Y Bazilevs. Isogeometric Analysis: Toward Integration of CAD and FEA. John Wiley & Sons; 2009.
[53] Grillanda N, Chiozzi A, Milani G, Tralli A. Metaheuristic algorithms for the kinematic limit analysis of masonry vaults. Submitted; 2019.
[54] SL Tilahun, HC Ong. Prey-predator algorithm: a new metaheuristic algorithm for optimization problems. Int J Inf Technol Decis Mak 2015;14:1331–1352. doi:10.1142/S021962201450031X.
[55] NTC2018. D.M. 17/01/2018 Aggiornamento delle «Norme tecniche per le costruzioni». S.O. alla G.U. n. 42 del 20/02/2018; 2018.
[56] CIRC2009. Instructions for the Application of the New Italian Building Code D.M. 14/01/2008. G.U. n. 47 26/02/2009; 2009 [in Italian].
[57] J DeLaine. The baths of Caracalla: a study in the design, construction, and economics of large-scale building projects in imperial Rome. J Roman Archaeol 1997.
[58] Simulia. Abaqus 6.11 User's Manual. Dassault Systemes; 2011.
[59] SR Ivancic. Numerical evaluation of the dynamic response of masonry heritage structures. University of Rochester; 2015.